Stability and Neimark–Sacker bifurcation analysis of a food-limited population model with a time delay*

Jiang Xiao-Wei(姜晓伟)[a], Guan Zhi-Hong(关治洪)[a]†, Zhang Xian-He(张先鹤)[b], Zhang Ding-Xue(张顶学)[c], and Liu Feng(刘 峰)[d]

[a] Department of Control Science and Engineering, Huazhong University of Science and Technology, Wuhan 430074, China
[b] College of Mechatronics and Control Engineering, Hubei Normal University, Huangshi 435002, China
[c] Petroleum Engineering College, Yangtze University, Jingzhou 434023, China
[d] Department of Electronic Information and Mechanics, China University of Geosciences, Wuhan 430074, China

(Received 11 June 2012; revised manuscript received 15 August 2012)

In this paper, a kind of discrete delay food-limited model obtained by the Euler method is investigated, where the discrete delay τ is regarded as a parameter. By analyzing the associated characteristic equation, the linear stability of this model is studied. It is shown that Neimark–Sacker bifurcation occurs when τ crosses certain critical values. The explicit formulae which determine the stability, direction, and other properties of bifurcating periodic solution are derived by means of the theory of center manifold and normal form. Finally, numerical simulations are performed to verify the analytical results.

Keywords: food-limited model, time delay, Neimark–Sacker bifurcation, periodic solution

PACS: 02.30.Ks, 02.30.Oz **DOI:** 10.1088/1674-1056/22/3/030204

1. Introduction

It is well known that the dynamic behavior (including stability, attractivity, persistence, periodic oscillation, bifurcation, and chaos) of the continuous-time model with or without a time delay have become a subject of intense research activities due to their promising potential applications in many fields such as signal processing, pattern recognition, optimization and associative memories. Some important results have been reported.[1–4] Syed[5] gave stability criteria for a class neural network with time-varying delays by using a new Lyapunov functional. The existence of the periodic solution for the nonlinear functional differential equation is obtained using the continuation theorem of the coincidence degree theory.[6] In particular, the bifurcation phenomenon can occur in parameter-dependent dynamic systems. When the parameters are varied, changes may occur in the qualitative structure of the solutions for certain parameter values. The properties of periodic solution arising from the Neimark–Sacker bifurcation are of great interest.

For experimental or computational purposes, it is common to discretize the continuous-time model. Certainly, the discrete-time analog inherits the dynamic characteristics of the continuous-time model under weak or no restrictions on the discretization step size, and also retains functionally similar to the continuous-time system and any physical or biological reality that the continuous-time model has. We follow Ref. [7] to discuss the importance and need for discrete-time analogs to reflect the dynamics of their continuous-time counterparts. Recent works by Jing *et al.*,[8] Liu and Xiao,[9] and Agiza *et al.*[10] also showed that, for the discrete-time models, the dynamics can produce more patterns than those observed in continuous-time models. Many authors considered the numerical approximation of a distributed delay differential equation undergoing a Neimark–Sacker bifurcation by using different numerical methods, such as the θ-method, Euler method, and Trapezoidal method.[11–13] A deep insight into the system dynamics can provide critical insight and guidance into the analysis and design of the control scheme from the viewpoint of dynamics and control theory.[14–16] For example, the authors in Ref. [17] obtained less conservative criteria for feedback control in a delayed dynamic system. In this paper, we apply the forward Euler scheme to discretize the delay differential equation

$$\dot{u}(t) = \frac{ru(t)(K - u(t-\tau))}{K + \gamma u(t-\tau)}, \ (\tau > 0). \tag{1}$$

Here, the population density is denoted by $u(t)$, γ is the ratio of the rate of increase with limited food to the rate of replacement of mass in the population at saturation, and the positive constants r and K represent the growth rate of the population and the carrying capacity of the habitat, respectively. Assuming that a growing population requires more food (growth and maintenance) than a saturated one (maintenance only), a further modification that the average growth rate is a function of some specified delayed argument $t - \tau$ is assumed. Taking the delay τ as the bifurcation parameter, we shall investigate the effect of the delay τ on the dynamics of the system (1).

*Project supported by the National Natural Science Foundation of China (Grant Nos. 61272069, 61272114, 61073026, 61170031, and 61100076).
†Corresponding author. E-mail: zhguan@mail.hust.edu.cn
© 2013 Chinese Physical Society and IOP Publishing Ltd

The organization of this paper is as follows. In Section 2, the stability of the positive equilibrium and the existence of Neimark–Sacker bifurcation are discussed. In Section 3, a formula for determining the direction of the Neimark–Sacker bifurcation and the stability of bifurcating periodic solutions will be given by using the theory of center manifold and norm form introduced by Hassard.[18] In Section 4, some parameters are chosen to illustrate the obtained analytical results. Section 5 draws a conclusion.

2. Stability analysis

In order to facilitate analysis, some transformations need to be given for system (1). Define a new variable as $x(t) = u(t\tau)$, then

$$\dot{x}(t) = \frac{\tau r x(t)(K - x(t-1))}{K + \gamma x(t-1)}. \tag{2}$$

The forward Euler scheme applied to Eq. (2) yields the delay difference equation

$$x_{n+1} = x_n + \frac{\tau r h x_n (K - x_{n-m})}{K + \gamma x_{n-m}}, \tag{3}$$

where the step size is $h = 1/m$ $(m = 1, 2, \ldots)$, and u_n is an approximate value of $u(nh)$ for sufficiently small h.

For all parameter values, the system has two fixed points $x^* = 0$ and $x^* = K$. From the point of view of biology, it will be more meaningful to study the local behavior of the positive fixed point $x^* = K$.

Now we study the stability of positive fixed points. Note that the local stability of a fixed point (x, y) is determined by the modules of eigenvalues of the characteristic equation at the fixed point.

Let $y_n = x_n - x^*$, then

$$y_{n+1} = y_n + \frac{\tau r h (y_n + x^*)[K - (y_{n-m} + x^*)]}{K + \gamma(y_{n-m} + x^*)}. \tag{4}$$

Thus, we study the stability of the fixed point $x^* = K$ of map (2), instead of studying the stability of the fixed point $y^* = 0$ of map (3). By introducing a new variable $\boldsymbol{Y}_n = (y_n, y_{n-1}, \ldots, y_{n-m})^{\mathrm{T}}$. We can rewrite Eq. (4) in the form

$$\boldsymbol{Y}_{n+1} = \boldsymbol{F}(\boldsymbol{Y}_n, \tau), \tag{5}$$

where $\boldsymbol{F} = (F_0, F_1, \ldots, F_m)^{\mathrm{T}}$, and

$$F_k = \begin{cases} y_n + \dfrac{\tau r h (y_n + x^*)[K - (y_{n-m} + x^*)]}{K + \gamma(y_{n-m} + x^*)}, & (k = 0), \\ y_{n-k+1}, & (1 \le k \le m). \end{cases}$$

Clearly, the origin is a fixed point of Eq. (5), and the linear part of Eq. (5) is $Y_{n+1} = AY_n$, in which

$$A = \begin{pmatrix} 1 & 0 & \cdots & 0 & \dfrac{-\tau r h}{1+\gamma} \\ 1 & 0 & \cdots & 0 & 0 \\ 0 & 1 & \cdots & 0 & 0 \\ \vdots & \vdots & \ddots & \vdots & \vdots \\ 0 & 0 & \cdots & 1 & 0 \end{pmatrix}_{(m+1)\times(m+1)}.$$

The characteristic equation of Eq. (5) evaluated at the fixed point $x^* = K$ can be written as

$$\lambda^{m+1} - \lambda^m + \frac{\tau r h}{1+\gamma} = 0. \tag{6}$$

It is well known that the stability of the zero equilibrium solution of Eq. (5) depends on the distribution of the zeros of the roots of Eq. (6). Ruan and Wei[19] gave the distributions of the roots of the transcendental functions which are characteristic equations of delay differential equations. In this paper, we will employ the results from Zhang *et al.*[13] to analyze the distribution of the zeros of the characteristic equation (6).

Lemma 1[13] Suppose that $\widehat{\boldsymbol{B}} \subset \mathbf{R}$ is a bound, closed, and connected set, and $f(\lambda, \tau) = \lambda^m + p_1(\tau)\lambda^{m-1} + p_2(\tau)\lambda^{m-2} + \cdots + p_m(\tau)$ is continuous in $(\lambda, \tau) \in C \times \widehat{\boldsymbol{B}}$ (τ is a parameter, $\tau \in \widehat{\boldsymbol{B}}$). Then, as τ varies, the sum of the order of the zeros of $f(\lambda, \tau)$ out of the unit circle

$$\{\lambda \in C : |\lambda| > 1\}$$

can change only if a zero appears on or crosses the unit circle.

Lemma 2 There exists $\bar{\tau} > 0$ such that for $0 < \tau < \bar{\tau}$ all roots of Eq. (6) have a modulus less than one.

Proof When $\tau = 0$, equation (6) becomes $\lambda^{m+1} - \lambda^m = 0$. The equation has an m-fold roots $\lambda = 0$, and simple root $\lambda = 1$.

Consider the root $\lambda(\tau)$ such that $|\lambda(0)| = 1$. This root depends continuously on τ and is a differential function of τ. Since the parameter values are all positive, it follows from Eq. (6) that

$$\begin{aligned} \frac{\mathrm{d}|\lambda|^2}{\mathrm{d}\tau}\Big|_{\tau=0,\lambda=1} &= \left[\lambda \frac{\mathrm{d}\bar{\lambda}}{\mathrm{d}\tau} + \bar{\lambda}\frac{\mathrm{d}\lambda}{\mathrm{d}\tau}\right]\Big|_{\tau=0,\lambda=1} \\ &= -\frac{rh}{1+\gamma} < 0. \end{aligned}$$

Consequently, $|\lambda| < 1$ holds for all sufficiently small $\tau > 0$. Thus, all roots of Eq. (6) lies in $|z| < 1$ for sufficiently small positive τ, and the existence of the maximal $\bar{\tau}$ follows. This completes the proof.

Assume that the step size h is sufficiently small, and let $\exp(\mathrm{i}\omega^*)$ be a root of Eq. (6) when $\tau = \tau^*$, then we have

$$\mathrm{e}^{\mathrm{i}(m+1)\omega^*} - \mathrm{e}^{\mathrm{i}m\omega^*} + \frac{\tau^* r h}{1+\gamma} = 0.$$

Separating the real and imaginary part, we have

$$\begin{aligned} &\cos((m+1)\omega^*) - \cos(m\omega^*) = -\frac{\tau^* r h}{1+\gamma}, \\ &\sin((m+1)\omega^*) - \sin(m\omega^*) = 0. \end{aligned} \tag{7}$$

Then, we derive from Eq. (7) that

$$\cos w^* = 1 - \frac{(\tau^* r h)^2}{2(1+\gamma)^2}.$$

In addition, we must notice that

$$\frac{\tau^* r h}{1+\gamma} = |\cos((m+1)\omega^*) - \cos(m\omega^*)| \le 2.$$

Consequently,

$$0 < \tau^* \le \frac{2(1+\gamma)}{rh}. \tag{8}$$

From the above analysis, the roots $\exp(\pm\mathrm{i}\omega^*)$ of Eq. (6) with

a modulus of one satisfy

$$\begin{cases} \cos\omega^* = 1 - \dfrac{(\tau^* rh)^2}{2(1+\gamma)^2}, \\ \tau^* = \dfrac{-(1+\gamma)[\cos((m+1)\omega^*) - \cos(m\omega^*)]}{rh}, \\ h = \dfrac{1}{m}. \end{cases} \tag{9}$$

Notice that there exist finite values of the time delay parameter, namely $\tau_0 < \tau_1 < \cdots < \tau_n$, satisfying Eq. (9) because of the constraint (8). From Eq. (9), some system parameters can be chosen to simulate the bifurcation behavior of the system. This completes the proof.

Lemma 3 For the given parameter values of the system, we have

$$\frac{\mathrm{d}|\lambda|^2}{\mathrm{d}\tau}\Big|_{\tau=\tau^*,\omega=\omega^*} = \left[\lambda\frac{\mathrm{d}\bar{\lambda}}{\mathrm{d}\tau} + \bar{\lambda}\frac{\mathrm{d}\lambda}{\mathrm{d}\tau}\right]\Big|_{\tau=\tau^*,\omega=\omega^*} > 0.$$

Proof According to the above analysis, we can obtain

$$\begin{aligned} \frac{\mathrm{d}|\lambda|^2}{\mathrm{d}\tau}\Big|_{\tau=\tau^*,\omega=\omega^*} &= \left[\lambda\frac{\mathrm{d}\bar{\lambda}}{\mathrm{d}\tau} + \bar{\lambda}\frac{\mathrm{d}\lambda}{\mathrm{d}\tau}\right]\Big|_{\tau=\tau^*,\omega=\omega^*} \\ &= \left[\lambda\frac{\tau rh}{K(1+\gamma)[(m+1)\bar{\lambda}^m - m\bar{\lambda}^{m-1}]} + \bar{\lambda}\frac{\tau rh}{K(1+\gamma)[(m+1)\lambda^m - m\lambda^{m-1}]}\right]\Big|_{\tau=\tau^*,\omega=\omega^*} \\ &= \frac{-rh[2(m+1)\cos((m+1)\omega^*) - 2m\cos(m\omega^*)]}{K(1+\gamma)[(m+1)^2 - 2m(m+1)\cos\omega^* + m^2]}. \end{aligned}$$

From Eq. (6), we have

$$\cos mw^* = \frac{\tau^* rh}{2K(1+\gamma)}, \quad \cos(m+1)w^* = -\frac{\tau^* rh}{2K(1+\gamma)},$$

and it is easy to see that

$$(m+1)^2 - 2m(m+1)\cos\omega^* + m^2 = 1 + 2m(m+1)(1-\cos\omega^*) > 0.$$

Then, we can obtain

$$\frac{\mathrm{d}|\lambda|^2}{\mathrm{d}\tau}|_{\tau=\tau^*,\omega=\omega^*} = \frac{-rh[2(m+1)\cos(m+1)\omega^* - 2m\cos(m\omega^*)]}{K(1+\gamma)[(m+1)^2 - 2m(m+1)\cos\omega^* + m^2]} = \frac{(2m+1)\tau^* r^2 h^2}{K^2(1+\gamma)^2[1+2m(m+1)(1-\cos\omega^*)]} > 0.$$

This completes the proof.

From Lemmas 1–3, we derive the following results on the stability and bifurcation of the system (5).

Theorem 1 For all defined system parameters, we have

(i) The positive equilibrium $x^* = K$ of system (3) is asymptotically stable for $\tau \in [0, \tau_0)$, and unstable for $\tau > \tau_0$.

(ii) The positive equilibrium $x^* = K$ of system (3) undergoes a Neimark–Sacker bifurcation when $\tau = \tau_0$. That is, system (3) has a branch of periodic solutions bifurcating from the positive equilibrium near $\tau = \tau_0$.

3. Direction and stability of the Neimark–Sacker bifurcation

Based on the analysis in Section 2, we will discuss the Neimark–Sacker bifurcation of the positive fixed point $x^* = K$ in this section. We choose parameter τ as a bifurcation parameter to study the Neimark–Sacker bifurcation of $x^* = K$ by using the center manifold theorem and normal form theory.

Without loss of generality, we denote the critical value τ_j $(j = 0, 1, \ldots, n)$ by τ^*, where system (5) undergoes a Neimark–Sacker bifurcation at the origin. For map (5), we have

$$\boldsymbol{Y}_{n+1} = \boldsymbol{A}\boldsymbol{Y}_n + \frac{1}{2}\boldsymbol{B}(\boldsymbol{Y}_n, \boldsymbol{Y}_n) + \frac{1}{6}\boldsymbol{C}(\boldsymbol{Y}_n, \boldsymbol{Y}_n, \boldsymbol{Y}_n) + o(\|\boldsymbol{Y}_n\|^4),$$

where

$$\begin{aligned} \boldsymbol{B}(\boldsymbol{Y}_n, \boldsymbol{Y}_n) &= (B_0(\boldsymbol{Y}_n, \boldsymbol{Y}_n), B_1(\boldsymbol{Y}_n, \boldsymbol{Y}_n), \ldots, B_m(\boldsymbol{Y}_n, \boldsymbol{Y}_n))^{\mathrm{T}}, \\ \boldsymbol{C}(\boldsymbol{Y}_n, \boldsymbol{Y}_n, \boldsymbol{Y}_n) &= (C_0(Y_n, Y_n, Y_n), C_1(\boldsymbol{Y}_n, \boldsymbol{Y}_n, \boldsymbol{Y}_n), \ldots, \\ &\quad C_m(\boldsymbol{Y}_n, \boldsymbol{Y}_n, \boldsymbol{Y}_n))^{\mathrm{T}}, \end{aligned}$$

and

$$B_i(x,y) := \sum_{j,k}^{n} \frac{\partial^2 F_i(y,\tau^*)}{\partial y_j \partial y_k} x_j y_k, \ (i = 0, 1, \ldots, m),$$

$$C_i(x,y,u) := \sum_{j,k,l}^{n} \frac{\partial^3 F_i(y,\tau^*)}{\partial y_j \partial y_k \partial y_l} x_j y_k u_l, \ (i = 0, 1, \ldots, m).$$

Thus, we can obtain

$$\begin{aligned} B_0(Y_n, Y_n) &= -\frac{\tau rh}{(1+\gamma)} y_n y_{n-m} - \frac{\tau rhK}{(1+\gamma)} y_{n-m} y_{n-m}, \\ C_0(Y_n, Y_n, Y_n) &= \frac{2\tau rh\gamma}{(1+\gamma)^2} y_n y_{n-m}^2 + \frac{2\tau rh\gamma K}{(1+\gamma)^2} y_{n-m}^3, \end{aligned}$$

and $B_k = 0$, and $C_k = 0$ $(1 \le k \le m)$.

Let $\boldsymbol{q}(\tau) \in \boldsymbol{C}^{m+1}$ be a complex eigenvector of $\boldsymbol{A}(\tau)$ corresponding to $\exp(\mathrm{i}\omega^*)$, then $\boldsymbol{A}(\tau)\boldsymbol{q}(\tau) = \exp(\mathrm{i}\omega^*)\boldsymbol{q}(\tau)$. Again, let $\boldsymbol{p}(\tau) \in \boldsymbol{C}^{m+1}$ be a complex eigenvector of the transposed matrix $\boldsymbol{A}^{\mathrm{T}}(\tau)$ corresponding to $\exp(-\mathrm{i}\omega^*)$, then

$\boldsymbol{A}(\tau)\boldsymbol{p}(\tau)=\exp(-\mathrm{i}\omega^*)\boldsymbol{p}(\tau)$. Note that $\boldsymbol{p}(\tau)$ and $\boldsymbol{q}(\tau)$ must satisfy the normalization condition $\langle \boldsymbol{p},\boldsymbol{q}\rangle=1$, where $\langle \boldsymbol{p},\boldsymbol{q}\rangle=\sum_{j=0}^{m}\bar{p}_j q_j$. Let $\boldsymbol{q}=(q_0,q_1,\ldots,q_m)^{\mathrm{T}}$ and $\boldsymbol{p}=(p_0,p_1,\ldots,p_m)^{\mathrm{T}}$. Via direct calculation, we obtain the following relationship: $q_j=\exp(\mathrm{i}\omega^*)q_{j+1}$, $(j=0,1,\ldots,m-1)$, and by setting $q_0=1$, we can obtain the value of $\boldsymbol{q}$. Similarly, the eigenvector $\boldsymbol{p}$ satisfies the following equality:

$$\begin{cases} p_0-\dfrac{\tau rh}{(1+\gamma)}p_{m+1}=\mathrm{e}^{-\mathrm{i}\omega^*}q_0,\\ p_j=\mathrm{e}^{-\mathrm{i}\omega^*}p_{j+1},\ (j=0,1,\ldots,m-1). \end{cases}$$

Therefore,

$$\boldsymbol{p}=\left(p_0,-\mathrm{e}^{\mathrm{i}m\omega^*}\frac{\tau rh}{(1+\gamma)}p_0,\ldots,-\mathrm{e}^{\mathrm{i}\omega^*}\frac{\tau rh}{(1+\gamma)}p_0\right)^{\mathrm{T}}.$$

Denote $\boldsymbol{T}^{\mathrm{c}}$ as a real eigenspace corresponding to $\exp(\pm\mathrm{i}\omega^*)$, which is two-dimensional and is spanned by $\{\mathrm{Re}(q),\mathrm{Im}(q)\}$; denote $\boldsymbol{T}^{\mathrm{s}}$ as a real eigenspace corresponding to all eigenvalues of $\boldsymbol{A}^{\mathrm{T}}$ other than $\exp(\pm\mathrm{i}\omega^*)$, which is $(m-1)$-dimensional.

For any $\boldsymbol{x}\in\mathrm{R}^{m+1}$, we have its decomposition $\boldsymbol{x}=z\boldsymbol{q}+\bar{z}\bar{\boldsymbol{q}}+\boldsymbol{y}$, where $z\in\boldsymbol{C}$, $z\boldsymbol{q}+\bar{z}\bar{\boldsymbol{q}}\in\boldsymbol{T}^{\mathrm{c}}$, $\boldsymbol{y}\in\boldsymbol{T}^{\mathrm{s}}$. The complex variable z can be viewed as a new coordinate on $\boldsymbol{T}^{\mathrm{c}}$ and $z=\langle \boldsymbol{p},\boldsymbol{x}\rangle$, $\boldsymbol{y}=\boldsymbol{x}-\langle \boldsymbol{p},\boldsymbol{x}\rangle\boldsymbol{q}-\langle\bar{\boldsymbol{p}},\boldsymbol{x}\rangle\bar{\boldsymbol{q}}$. In this coordinate, the map F has the form

$$\begin{aligned} z&\mapsto \mathrm{e}^{\mathrm{i}\omega^*}z+\langle \boldsymbol{p},F(z\boldsymbol{q}+\bar{z}\bar{\boldsymbol{q}}+\boldsymbol{y})\rangle,\\ \boldsymbol{y}&\mapsto \boldsymbol{A}\boldsymbol{y}+F(z\boldsymbol{q}+\bar{z}\bar{\boldsymbol{q}}+\boldsymbol{y})-\langle \boldsymbol{p},F(z\boldsymbol{q}+\bar{z}\bar{\boldsymbol{q}}+\boldsymbol{y})\rangle\boldsymbol{q}\\ &\quad-\langle\bar{\boldsymbol{p}},F(z\boldsymbol{q}+\bar{z}\bar{\boldsymbol{q}}+\boldsymbol{y})\rangle\bar{\boldsymbol{q}}. \end{aligned}$$

Using Taylor expansions, we have

$$\begin{aligned} z&\mapsto \mathrm{e}^{\mathrm{i}\omega^*}z+\frac{1}{2}g_{20}z^2+g_{11}z\bar{z}+\frac{1}{2}g_{02}\bar{z}^2+\frac{1}{2}G_{21}z^2\bar{z}\\ &\quad+\langle G_{10},y\rangle cz+\langle G_{01},y\rangle\bar{z},\\ \boldsymbol{y}&\mapsto A\boldsymbol{y}+\frac{1}{2}H_{20}z^2+H_{11}z\bar{z}+\frac{1}{2}H_{02}\bar{z}^2+o(|z|^3), \end{aligned}\tag{10}$$

where $g_{ij}\in\boldsymbol{C}$, $G_{10},G_{01}\in\boldsymbol{C}^{m+1}$, and

$$\begin{aligned} &g_{20}=\langle \boldsymbol{p},\boldsymbol{B}(\boldsymbol{q},\boldsymbol{q})\rangle,\ g_{11}=\langle \boldsymbol{p},\boldsymbol{B}(\boldsymbol{q},\bar{\boldsymbol{q}})\rangle,\ g_{02}=\langle \boldsymbol{p},\boldsymbol{B}(\bar{\boldsymbol{q}},\bar{\boldsymbol{q}})\rangle,\\ &G_{21}=\langle \boldsymbol{p},C(\boldsymbol{q},\boldsymbol{q},\bar{\boldsymbol{q}})\rangle,\langle G_{10},\boldsymbol{y}\rangle=\langle \boldsymbol{p},\boldsymbol{B}(\boldsymbol{q},\boldsymbol{y})\rangle\rangle,\langle G_{01},\boldsymbol{y}\rangle\\ &\quad=\langle \boldsymbol{p},\boldsymbol{B}(\bar{\boldsymbol{q}},\boldsymbol{y})\rangle\\ &H_{20}=\boldsymbol{B}(\boldsymbol{q},\boldsymbol{q})-\langle \boldsymbol{p},\boldsymbol{B}(\boldsymbol{q},\boldsymbol{q})\rangle\boldsymbol{q}-\langle\bar{\boldsymbol{p}},\boldsymbol{B}(\boldsymbol{q},\boldsymbol{q})\rangle\bar{\boldsymbol{q}},\\ &H_{11}=\boldsymbol{B}(\boldsymbol{q},\bar{\boldsymbol{q}})-\langle \boldsymbol{p},\boldsymbol{B}(\boldsymbol{q},\bar{\boldsymbol{q}})\rangle\boldsymbol{q}-\langle\bar{\boldsymbol{p}},\boldsymbol{B}(\boldsymbol{q},\bar{\boldsymbol{q}})\rangle\bar{\boldsymbol{q}},\\ &H_{02}=\boldsymbol{B}(\bar{\boldsymbol{q}},\bar{\boldsymbol{q}})-\langle \boldsymbol{p},\boldsymbol{B}(\boldsymbol{q},\bar{\boldsymbol{q}})\rangle\boldsymbol{q}-\langle\bar{\boldsymbol{p}},\boldsymbol{B}(\bar{\boldsymbol{q}},\bar{\boldsymbol{q}})\rangle\bar{\boldsymbol{q}}. \end{aligned}$$

Now, we seek the center manifold which has the representation

$$\boldsymbol{y}=\boldsymbol{V}(z,\bar{z})=\frac{1}{2}w_{20}z^2+w_{11}z\bar{z}+\frac{1}{2}w_{02}\bar{z}^2+o(|z|^3),\tag{11}$$

where $\langle \boldsymbol{q}^*,w_{ij}\rangle=0$. Substituting Eq. (11) into Eq. (10), we have

$$\begin{cases} w_{20}=(\mathrm{e}^{2\mathrm{i}\omega^*}\boldsymbol{I}-\boldsymbol{A})^{-1}H_{20},\\ w_{11}=(\boldsymbol{I}-\boldsymbol{A})^{-1}H_{11},\\ w_{02}=(\mathrm{e}^{-2\mathrm{i}\omega^*}\boldsymbol{I}-\boldsymbol{A})^{-1}H_{02}. \end{cases}$$

The Taylor coefficients can be expressed by the following formulae $g_{20}=\langle \boldsymbol{p},\boldsymbol{B}(\boldsymbol{q},\boldsymbol{q})\rangle$, $g_{11}=\langle \boldsymbol{p},\boldsymbol{B}(\boldsymbol{q},\bar{\boldsymbol{q}})\rangle$, $g_{02}=\langle \boldsymbol{p},\boldsymbol{B}(\bar{\boldsymbol{q}},\bar{\boldsymbol{q}})\rangle$, and

$$\begin{aligned} g_{21}&=\langle \boldsymbol{p},\boldsymbol{C}(\boldsymbol{q},\boldsymbol{q},\bar{\boldsymbol{q}})\rangle-2\langle \boldsymbol{p},\boldsymbol{B}(\boldsymbol{q},(\boldsymbol{I}-\boldsymbol{A})^{-1}\boldsymbol{B}(\boldsymbol{q},\bar{\boldsymbol{q}}))\rangle\\ &\quad+\langle \boldsymbol{p},\boldsymbol{B}(\bar{\boldsymbol{q}},(\mathrm{e}^{2\mathrm{i}\omega^*}\boldsymbol{I}-\boldsymbol{A})^{-1}\boldsymbol{B}(\boldsymbol{q},\boldsymbol{q}))\rangle\\ &\quad+\frac{\mathrm{e}^{-i\omega^*}(1-2\mathrm{e}^{2\mathrm{i}\omega^*})}{1-\mathrm{e}^{-\mathrm{i}\omega^*}}\langle p,B(q,q)\rangle\\ &\quad\times\langle p,B(q,\bar{q})\rangle-\frac{2}{1-\mathrm{e}^{-\mathrm{i}\omega^*}}|\langle p,B(\bar{q},\bar{q})\rangle|^2\\ &\quad-\frac{\mathrm{e}^{\mathrm{i}\omega^*}}{\mathrm{e}^{3\mathrm{i}\omega^*}-1}|\langle p,B(\bar{q},\bar{q})\rangle|^2. \end{aligned}$$

Define

$$c_1(\tau)=\frac{g_{20}g_{11}(\bar{z}-3+2z)}{2(z^2-2)(\bar{z}-1)}+\frac{|g_{11}|^2}{1-\bar{z}}+\frac{|g_{02}|^2}{2(z^2-\bar{z})}+\frac{g_{21}}{2}.\tag{12}$$

Substituting $z=\mathrm{e}^{-\mathrm{i}\omega^*}$ into Eq. (12), we can obtain $c_1(\tau^*)$.

Theorem 2 The direction and stability of Neimark–Sacker bifurcation of Eq. (5) is determined by the sign of

$$l=-\frac{\mathrm{Re}[\exp(\mathrm{i}\omega^*)c_1(\tau^*)]}{d_h}.$$

If $l>0$ (<0), then the Neimark–Sacker bifurcation is supercritical (subcritical) and a unique closed invariant curve exists for $\tau>\tau^*$. The sign of $\mathrm{Re}[\mathrm{e}^{-\mathrm{i}\omega^*}c_1(\tau^*)]$ determines the stability of the closed invariant curve: the bifurcation closed invariant curve is orbitally stable (unstable) if $\mathrm{Re}[\exp(-\mathrm{i}\omega^*)c_1(\tau^*)]<0\ (>0)$.

4. Numerical simulations

To illustrate the analytical results obtained, let us consider the following particular case. Let $\gamma=0.2$, $r=2.4$, $K=2$, and $m=20$. Then $\tau_0=0.7763$ is the critical value at which the Neimark–Sacker bifurcation occurs. Figures 1–3 are the waveform plots and phase portraits of Eq. (3) when the step size $h=0.05$.

In Fig. 1, we show the waveform plot and phase portrait for Eq. (3) with initial value $x_n=1.6$ $(n=1,2,\ldots,21)$ when $\tau(=0.5)$ is smaller than $\tau_0(=0.7763)$. The equilibrium $x^*=2$ of Eq. (3) is asymptotically stable. In Figs. 2 and 3, we show the waveform plot and phase portrait for Eq. (3) with initial value $x_n=1.6$ $(n=1,2,\ldots,21)$ and $x_n=4.6$ $(n=1,2,\ldots,21)$, respectively. The equilibrium $x^*=2$ of Eq. (3) is unstable for $\tau(=0.8)$ and is smaller than $\tau_0(=0.7763)$. When τ varies and exceeds $\tau_0=0.7763$, the equilibrium loses its stability, and a unique and stable closed invariant curve bifurcates from the equilibrium for $\tau(=0.8)$ is smaller than $\tau_0(=0.7763)$. That is to say, the delay difference (Eq. (3)) has a Neimark–Sacker bifurcation at τ_0 when the step size h is sufficiently small. We should also notice that the initial condition has an important influence on the dynamic behavior of the system.

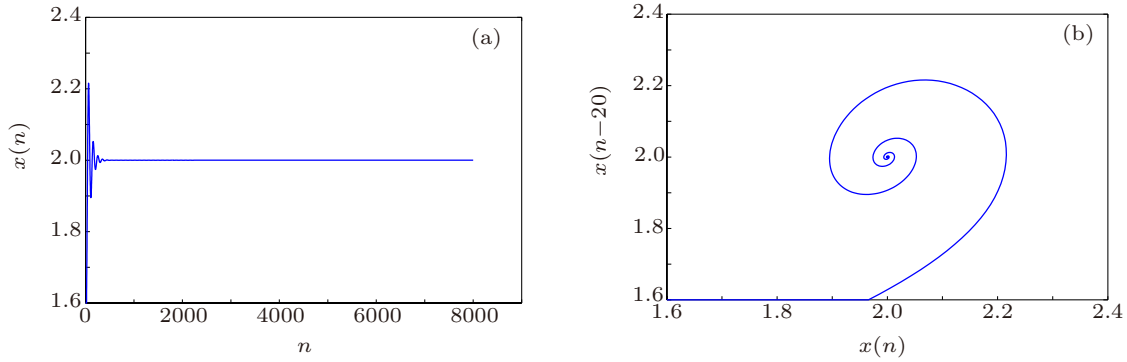


Fig. 1. (color online) (a) The equilibrium $x^* = 2$ is asymptotically stable for $\tau = 0.5$ when $h = 0.05$, $m = 20$, $r = 2.4$, $\gamma = 0.2$, and $K = 2$. (b) Corresponding phase portrait on the plane $(x(n), x(n-20))$ for $\tau = 0.5$.

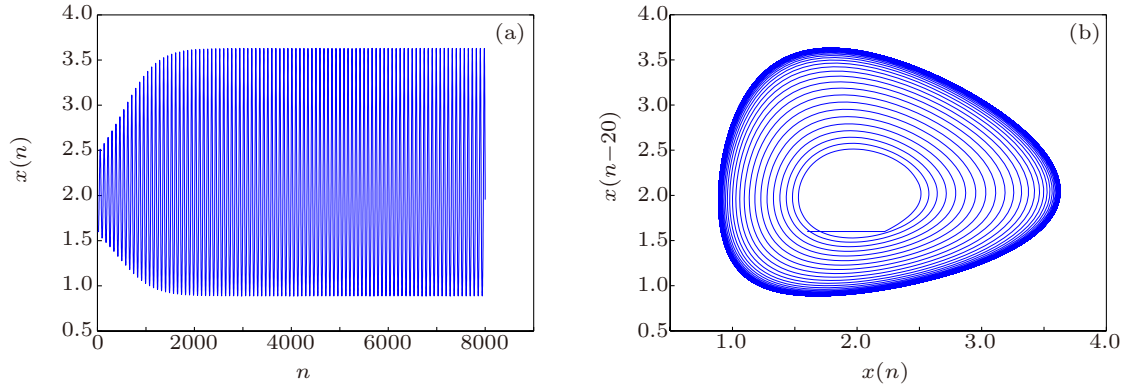


Fig. 2. (color online) (a) Waveform plot of Eq. (3) for $\tau\,(=0.8)$ (higher than $\tau_0 = 0.7763$) with initial value $x_n = 1.6$. (b) The stable closed invariant curve on the plane $x(n), x(n-20)$ when $\tau\,(=0.8)$ (greater than $\tau_0 = 0.7763$).

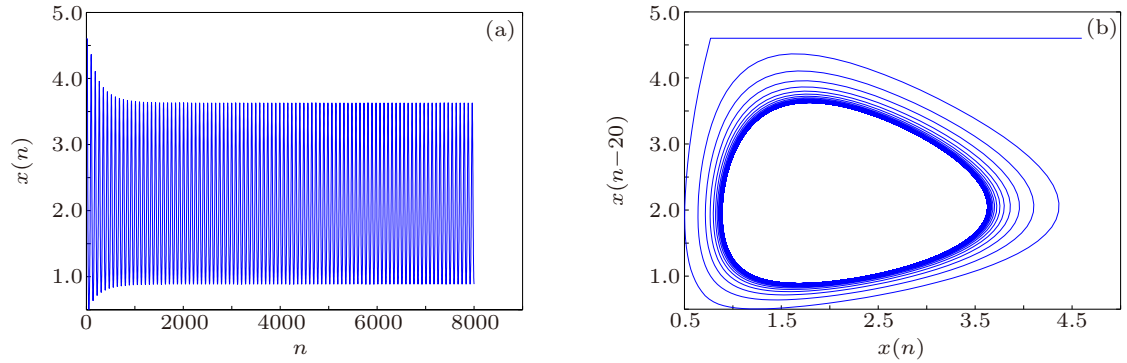


Fig. 3. (color online) (a) Waveform plot of Eq. (3) for $\tau = 0.8$ (great than $\tau_0 = 0.7763$) with initial value $x_n = 4.6$. (b) The stable closed invariant curve on the plane $x(n), x(n-20)$ when $\tau = 0.8$ (greater than $\tau_0 = 0.7763$).

5. Conclusion

In this paper, based on eigenvalue theory, the stability of a food-limited population model with a time delay has been investigated, and the parameter condition when Neimark–Sacker occurs is determined. The results about the direction and stability of Neimark–Sacker bifurcation have been obtained by means of the center manifold theorem and the normal form theory. Computer simulations are performed to illustrate the analytical results by choosing the values of some parameters.

References

[1] Li N, Sun H Y and Zhang Q L 2012 *Chin. Phys. B* **21** 010503
[2] He W L, Qian F, Cao J D and Han Q L 2011 *Phys. Lett. A* **375** 498
[3] Xiao M, Cao J D and Zheng W X 2011 *J. Franklin Inst.* **348** 2647
[4] Liu X Y and Sun J X 2012 *Nonlinear Anal. TMA* **75** 7
[5] Syed A M 2012 *Chin. Phys. B* **21** 070207
[6] Wang N 2012 *Chin. Phys. B* **21** 010202
[7] Mohamad S and Naim A 2002 *J. Comput. Appl. Math.* **138** 1
[8] Vilone D, Robledo A and Sanchez A 2011 *Phys. Rev. Lett.* **107** 038101
[9] Liu X and Xiao D M 2007 *Chaos Soliton. Fract.* **32** 80
[10] Agiza H, Elabbasy E, Elmetwally H and Elsadany A 2009 *Nonlinear Anal. RWA* **10** 116
[11] He Z M and Lai X 2011 *Nonlinear Anal. RWA* **12** 403
[12] Han W and Liu M X 2011 *Appl. Math. Comput.* **217** 5449
[13] Zhang C, Liu M and Zheng B 2003 *Appl. Math. Comput.* **146** 335
[14] Liu N, Guan Z H and Zhang H 2009 *Chin. Phys. B* **18** 1769
[15] Liu F, Guan Z H and Wang H O 2008 *Chin. Phys. B* **17** 2405
[16] Guan Z H, Liu F, Li J and Wang Y W 2012 *Chaos* **22** 023137
[17] Ye Z Y, Deng C B and Yang G 2011 *Chin. Phys. B* **20** 010207
[18] Hassard B, Kazarinoff D and Wan Y 1981 *Theory and Applications of Hopf Bifurcation* (Cambridge: Cambridge University Press)
[19] Ruan S and Wei J 2003 *Dynam. Cont. Dis. SER. A* **10** 863